



*Citation for published version:*

Wang, Z, Belardi, W, Yu, F, Wadsworth, WJ & Knight, JC 2014, 'Efficient diode-pumped mid-infrared emission from acetylene-filled hollow-core fiber', *Optics Express*, vol. 22, no. 18, pp. 21872-21878.  
<https://doi.org/10.1364/OE.22.021872>

*DOI:*

[10.1364/OE.22.021872](https://doi.org/10.1364/OE.22.021872)

*Publication date:*

2014

*Document Version*

Publisher's PDF, also known as Version of record

[Link to publication](#)

This paper was published in *Optics Express* and is made available as an electronic reprint with the permission of OSA. The paper can be found at the following URL on the OSA website: <http://dx.doi.org/10.1364/OE.22.021872> Systematic or multiple reproduction or distribution to multiple locations via electronic or other means is prohibited and is subject to penalties under law.

## University of Bath

### General rights

Copyright and moral rights for the publications made accessible in the public portal are retained by the authors and/or other copyright owners and it is a condition of accessing publications that users recognise and abide by the legal requirements associated with these rights.

### Take down policy

If you believe that this document breaches copyright please contact us providing details, and we will remove access to the work immediately and investigate your claim.

# Efficient diode-pumped mid-infrared emission from acetylene-filled hollow-core fiber

Zefeng Wang,<sup>1,2,\*</sup> Walter Belardi,<sup>1</sup> Fei Yu,<sup>1</sup> William J. Wadsworth,<sup>1</sup>  
and Jonathan C. Knight<sup>1</sup>

<sup>1</sup>Centre for Photonics and Photonic Materials, Department of Physics, University of Bath, Bath, BA2 7AY, UK

<sup>2</sup>College of Optoelectronic Science and Engineering, National University of Defense Technology, Changsha, 410073, China

\*hotrosemaths@163.com

**Abstract:** We report 3.1-3.2  $\mu\text{m}$  mid-infrared emission from acetylene-filled low loss antiresonant hollow-core fiber pumped with an amplified, modulated, narrowband, tunable 1.5  $\mu\text{m}$  diode laser. The maximum power conversion efficiency of  $\sim 30\%$ , with respect to the absorbed pump power, is obtained with a 10.5 m length of fiber at 0.7 mbar. The maximum efficiency with respect to the total incident pump power ( $\sim 20\%$ ) and the minimum pump laser energy required ( $< 50$  nJ) are both improved compared to similar work reported previously using an optical parametric oscillator as a pump source. This paper provides an effective route to obtain compact mid-infrared fiber lasers.

©2014 Optical Society of America

**OCIS codes:** (060.3510) Lasers, fiber; (140.3070) Infrared and far-infrared lasers; (140.4130) Molecular gas lasers; (060.5295) Photonic crystal fibers.

---

## References and links

1. Y. Kalisky and O. Kalisky, "The status of high-power lasers and their applications in the battlefield," *Opt. Eng.* **49**(9), 091003 (2010).
2. C. Carbonnier, H. Tobben, and U. B. Unrau, "Room temperature CW fiber laser at 3.22  $\mu\text{m}$ ," *Electron. Lett.* **34**(9), 893–894 (1998).
3. J. Li, D. D. Hudson, and S. D. Jackson, "High-power diode-pumped fiber laser operating at 3  $\mu\text{m}$ ," *Opt. Lett.* **36**(18), 3642–3644 (2011).
4. S. D. Jackson, "Towards high-power mid-infrared emission from a fiber laser," *Nat. Photonics* **6**(7), 423–431 (2012).
5. M. Bernier, V. Fortin, N. Caron, M. El-Amraoui, Y. Messaddeq, and R. Vallée, "Mid-infrared chalcogenide glass Raman fiber laser," *Opt. Lett.* **38**(2), 127–129 (2013).
6. O. Henderson-Sapir, J. Munch, and D. J. Ottaway, "Mid-infrared fiber lasers at and beyond 3.5  $\mu\text{m}$  using dual-wavelength pumping," *Opt. Lett.* **39**(3), 493–496 (2014).
7. M. Bernier, V. Fortin, M. El-Amraoui, Y. Messaddeq, and R. Vallée, "3.77  $\mu\text{m}$  fiber laser based on cascaded Raman gain in a chalcogenide glass fiber," *Opt. Lett.* **39**(7), 2052–2055 (2014).
8. T. Y. Chang and O. R. Wood, "An optically pumped CO<sub>2</sub> laser," *IEEE J. Quantum Electron.* **8**(6), 598 (1972).
9. H. R. Schlossberg and H. R. Fetterman, "Optically pumped vibrational transition laser in OCS," *Appl. Phys. Lett.* **26**(6), 316–318 (1975).
10. H. C. Miller, D. T. Radzykewycz, and G. Hager, "An optically pumped mid-infrared HBr laser," *IEEE J. Quantum Electron.* **30**(10), 2395–2400 (1994).
11. J. E. McCord, H. C. Miller, G. Hager, A. I. Lampron, and P. G. Crowell, "Experimental investigation of an optically pumped mid-infrared carbon monoxide laser," *IEEE J. Quantum Electron.* **35**(11), 1602–1612 (1999).
12. C. S. Kletecka, N. Campbell, C. R. Jones, J. W. Nicholson, and W. Rudolph, "Cascade lasing of molecular HBr in the four micron region pumped by a Nd:YAG laser," *IEEE J. Quantum Electron.* **40**(10), 1471–1477 (2004).
13. T. Ehrenreich, B. Zhdanov, T. Takekoshi, S. P. Phipps, and R. J. Knize, "Diode pumped cesium laser," *Electron. Lett.* **41**(7), 415–416 (2005).
14. A. V. V. Nampoothiri, A. Ratanavis, N. Campbell, and W. Rudolph, "Molecular C<sub>2</sub>H<sub>2</sub> and HCN lasers pumped by an optical parametric oscillator in the 1.5- $\mu\text{m}$  band," *Opt. Express* **18**(3), 1946–1951 (2010).
15. R. F. Cregan, B. J. Mangan, J. C. Knight, T. A. Birks, P. St. J. Russell, P. J. Roberts, and D. C. Allan, "Single-mode photonic band gap guidance of light in air," *Science* **285**(5433), 1537–1539 (1999).
16. F. Benabid, J. C. Knight, G. Antonopoulos, and P. St. J. Russell, "Stimulated Raman scattering in hydrogen-filled hollow-core photonic crystal fiber," *Science* **298**(5592), 399–402 (2002).
17. F. Benabid, G. Bouwmans, J. C. Knight, P. St. J. Russell, and F. Couny, "Ultrahigh efficiency laser wavelength conversion in a gas-filled hollow core photonic crystal fiber by pure stimulated rotational Raman scattering in molecular hydrogen," *Phys. Rev. Lett.* **93**(12), 123903 (2004).

18. F. Couny, F. Benabid, P. J. Roberts, P. S. Light, and M. G. Raymer, "Generation and photonic guidance of multi-octave optical-frequency combs," *Science* **318**(5853), 1118–1121 (2007).
19. B. Beaudou, F. Couny, Y. Y. Wang, P. S. Light, N. V. Wheeler, F. Gérôme, and F. Benabid, "Matched cascade of bandgap-shift and frequency-conversion using stimulated Raman scattering in a tapered hollow-core photonic crystal fibre," *Opt. Express* **18**(12), 12381–12390 (2010).
20. A. M. Jones, A. V. Nampoothiri, A. Ratanavis, T. Fiedler, N. V. Wheeler, F. Couny, R. Kadel, F. Benabid, B. R. Washburn, K. L. Corwin, and W. Rudolph, "Mid-infrared gas filled photonic crystal fiber laser based on population inversion," *Opt. Express* **19**(3), 2309–2316 (2011).
21. A. M. Jones, C. Fourcade-Dutin, C. Maoc, B. Baumgart, A. V. V. Nampoothiric, N. Campbell, Y. Wang, F. Benabid, W. Rudolph, B. R. Washburn, and K. L. Corwin, "Characterization of mid-infrared emissions from C<sub>2</sub>H<sub>2</sub>, CO, CO<sub>2</sub>, and HCN-filled hollow fiber lasers," *Proc. SPIE* **8237**, 82373Y (2012).
22. A. V. Vasudevan Nampoothiri, A. M. Jones, C. Fourcade-Dutin, C. Mao, N. Dadashzadeh, B. Baumgart, Y. Y. Wang, M. Alharbi, T. Bradley, N. Campbell, F. Benabid, B. R. Washburn, K. L. Corwin, and W. Rudolph, "Hollow-core optical fiber gas lasers (HOFGLAS): a review (Invited)," *Opt. Mater. Express* **2**(7), 948–961 (2012).
23. B. M. Trabold, A. Abdolvand, T. G. Euser, and P. St. J. Russell, "Efficient anti-Stokes generation via intermodal stimulated Raman scattering in gas-filled hollow-core PCF," *Opt. Express* **21**(24), 29711–29718 (2013).
24. Z. Wang, F. Yu, W. Wadsworth, and J. C. Knight, "1.9  $\mu\text{m}$  coherent source generation in hydrogen-filled hollow core fiber by stimulated Raman scattering," *Optical Fiber Communication Conference, San Francisco, United States, 2014*.
25. F. Yu, W. J. Wadsworth, and J. C. Knight, "Low loss silica hollow core fibers for 3-4  $\mu\text{m}$  spectral region," *Opt. Express* **20**(10), 11153–11158 (2012).
26. F. Yu and J. C. Knight, "Spectral attenuation limits of silica hollow core negative curvature fiber," *Opt. Express* **21**(18), 21466–21471 (2013).
27. A. N. Kolyadin, A. F. Kosolapov, A. D. Pryamikov, A. S. Biriukov, V. G. Plotnichenko, and E. M. Dianov, "Light transmission in negative curvature hollow core fiber in extremely high material loss region," *Opt. Express* **21**(8), 9514–9519 (2013).
28. W. Belardi and J. C. Knight, "Hollow antiresonant fibers with low bending loss," *Opt. Express* **22**(8), 10091–10096 (2014).
29. A. E. Siegman, *Lasers* (University Science Books, Sausalito California, 1986).
30. W. C. Swann and S. L. Gilbert, "Pressure-induced shift and broadening of 1510-1540 nm acetylene wavelength calibration lines," *J. Opt. Soc. Am. B* **17**(7), 1263–1270 (2000).
31. C. N. Banwell, *Fundamentals of Molecular Spectroscopy* (McGraw-Hill Book Company Limited, London, 1972).

---

## 1. Introduction

Fiber lasers have wide potential applications, and are increasingly replacing traditional solid state and gas lasers in many applications [1] due to their compactness, high efficiencies, excellent beam qualities and convenient heat management. Compact mid-infrared (mid-IR) fiber lasers have wide application in defense, security, atmosphere monitoring, and medicine, and have attracted enormous attention [2–7]. Usually, due to the low damage threshold, solid-core fiber lasers lack the ability to provide the same power levels as conventional gas lasers, which can reach MW levels in chemical gas lasers [1]. Because of nonlinear effects, the spectral linewidth of light generated in glass fibers will broaden at high powers. As the number of rare earth materials is limited, only certain laser wavelengths are available. Mid-IR fiber lasers are usually generated in erbium-doped or holmium-doped glass fibers. A CW 3.22  $\mu\text{m}$  laser was generated in holmium-doped fluorozirconate fiber [2]. Gas lasers have been demonstrated to be an effective method to generate mid-IR emission [8–14]. In traditional gas cells the effective interaction length is very short and the system can be bulky and cumbersome, limiting the applications of these lasers. The advent of hollow core photonic crystal fibers (HC-PCF) and their properties of long effective interaction length, high optical confinement, and the possibility of control of the effective gain spectrum make it possible to develop a novel type of laser, fiber gas lasers, which combines the advantages of both fiber and gas lasers [15, 16]. By properly designing the transmission bands of HC-PCF, selecting active gases and pump sources, fiber gas lasers can potentially provide a wide range of emission wavelengths from the UV to the IR. Owing to the nature of transitions in atomic and molecular gases, fiber gas lasers are spectrally narrow even without additional linewidth limiting measures. Since the first emission in H<sub>2</sub>-filled HC-PCF by stimulated Raman scattering was demonstrated in 2002 [16], fiber gas lasers have been intensively investigated [17–24]. The first mid-IR fiber gas laser was demonstrated in acetylene-filled Kagome structured hollow core fiber in 2011 [20], but the measured slope efficiency was only ~1%

because of the high transmission loss of 20 dB/m at laser wavelength. By optimizing the fiber structure, the loss was greatly improved to  $\sim 5$  dB/m, but the power conversion efficiency with the respect to the total incident pump laser power was still low ( $<10\%$ ) [21,22] due to the broad linewidth of the pump source of optical parametric oscillator (OPO). The OPO is bulky and cumbersome, and not suitable for compact laser designs. Recently, we have characterized a type of HC-PCF with anti-resonant core walls [25–28] guiding light into the mid-infrared with low loss (minimum loss  $\sim 0.034$  dB/m at 3050 nm). However, the use of very low-loss fiber is not critical in this experiment due to the freedom to adjust the gas concentration and the high optical gain which is attainable. A loss of a few dB/m at the output wavelength is low enough to enable high conversion efficiency with suitable gas pressure and fiber length. Dramatically reducing the fiber loss to  $<0.1$  dB/m does not appreciably increase the maximum conversion efficiency, but does allow longer fiber lengths which increases the maximum output pulse energy while maintaining the low gas pressures which give the highest efficiency.

Here we use this type of hollow core fiber to demonstrate mid-IR emission from acetylene pumped with an amplified, modulated, narrowband, tunable diode laser. Efficient mid-IR emission at 3.12  $\mu\text{m}$  and 3.16  $\mu\text{m}$  is observed when the diode laser is precisely tuned to the resonance with the absorption line of  $^{12}\text{C}_2\text{H}_2$  at  $\lambda = 1530.37$  nm. The use of a narrow linewidth pump source improves the total optical-to-optical conversion efficiency as it is better matched to the molecular absorption linewidth. As a result, a maximum power conversion efficiency of  $\sim 30\%$  with respect to the absorbed pump pulse energy, and 20% relative to the total incident pump energy, was obtained using a 10.5 m fiber length, with 4.2  $\mu\text{J}$  total incident pump energy, and 0.7 mbar acetylene pressure. The efficiency is close to the theoretical limit value of 33% for this kind of acetylene laser system, which arises from the simultaneous saturation of pump and lasing transitions [22].

## 2. Experimental setup

### 2.1 Anti-resonant HC-PCF

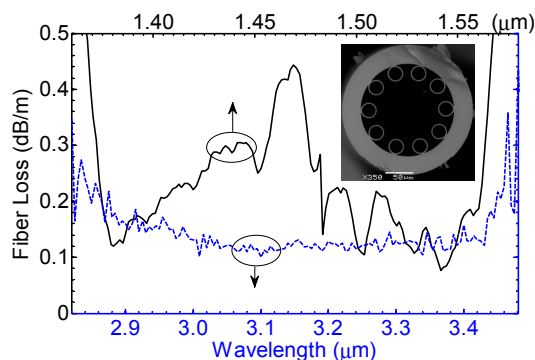


Fig. 1. The measured transmission loss of the anti-resonant HC-PCF at shorter (solid line, top x-axis) and longer (dash line, bottom x-axis) wavelength, *inset*: Scanning electron micrograph of the test fiber.

The hollow core fiber used here [28] is of the design shown in the insert of Fig. 1. It has a core diameter of  $\sim 109$   $\mu\text{m}$ , an outer diameter of  $\sim 233$   $\mu\text{m}$ , an average “cladding tube” diameter of 27.9  $\mu\text{m}$ , and a silica wall thickness of  $\sim 2.4$   $\mu\text{m}$ . The length used in the experiments is 10.5 m, which we determined to be the optimum length through trial and error. The transmission loss was measured by the standard cut-back method using a tungsten halogen lamp as the light source, and the results are shown in Fig. 1. We can see that the loss at the pump wavelength of 1.53  $\mu\text{m}$  is  $\sim 0.11$  dB/m; the loss around 3.1–3.2  $\mu\text{m}$ , near the laser wavelengths, is  $\sim 0.1$  dB/m. Although the core diameter is large, this fiber has a low bending

loss of 0.15 dB/turn at 3.1  $\mu\text{m}$  with a bending diameter of 16 cm [28]. Therefore, the fiber could be coiled with a reasonably small diameter ( $\sim 30$  cm) in experiments.

## 2.2 Modulated, amplified, tunable pump diode laser

The modulated, amplified tunable pump diode laser is shown in Fig. 2. We modulate the tunable CW laser (*ID Photonics GMBH*, CoBrite DX1, linewidth  $< 100$  kHz, maximum output power  $\sim 40$  mW) using two Mach-Zehnder intensity modulators (*Thorlabs*, LN56S-FC, 10 GHz) and a semiconductor optical amplifier (SOA, *Thorlabs* S9FC1004P). Here the SOA is used as an optical switch to suppress the low level CW which is transmitted by intensity modulator 1, and becomes significant for low pulse repetition rates. Two fiber polarization controllers (FPC) are used before the SOA and the second modulator respectively. All the modulators are driven by the same delay generator (*Stanford Research Systems* DG 645) with proper time delays. Two stages of erbium-doped fiber amplifiers (EDFA) are used. A 60 cm highly doped fiber (*Thorlabs* ER110-4/125) is used as a pre-amplifier, backward pumped with a 980 nm laser diode, whilst a 6 m doped fiber (*Thorlabs* ER16-8/125) is used as a power-amplifier, backward pumped with a 1483 nm laser diode. To protect the optical components and avoid self-excited oscillations in the EDFAs, several optical isolators are used.

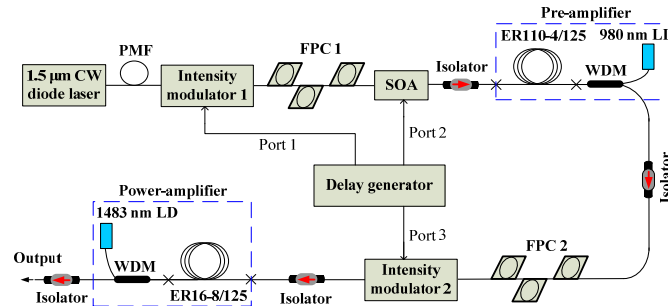


Fig. 2. The modulated, amplified pump diode laser setup. CW: Continuous wave; PMF: Polarization-maintaining fiber; FPC: Fiber polarization controller; SOA: Semiconductor optical amplifier; WDM: Wavelength division multiplexer; LD: Laser diode.

We used the absorption line P(9) as the pump transition, as shown in Fig. 5. We used a pump modulation frequency of 10 kHz and pulse duration of 20 ns. The maximum average output power of the pump source was about 50 mW. The CW diode laser was very stable both in power (measured fluctuation  $< \pm 2.5\%$  in 5 hours) and frequency (measured shift  $< 100$  MHz in 10 hours), so analog closed-loop wavelength control system for the pump laser was not necessary. To evaluate the linewidth of the modulated, amplified pump diode laser, the absorption linewidth of acetylene was measured by tuning the frequency across the absorption line and measuring the transmitted power. The results are shown in Fig. 3, where the central wavelength is 1530.37 nm. The measured absorption linewidth in 10.5 m hollow core fiber filled with 1.33 mbar acetylene (natural isotope content) using the unamplified CW diode laser is  $\sim 460$  MHz, which is in agreement with the Doppler broadening of  $\sim 480$  MHz (for  $^{12}\text{C}_2\text{H}_2$ , room temperature, central wavelength 1.53  $\mu\text{m}$ ) [29]. The absorption linewidth in a reference gas cell (*Photonics Technology*, length 50 mm, diameter 10 mm,  $^{12}\text{C}_2\text{H}_2$  purity  $> 99\%$ , pressure 22.7 mbar) is measured to be  $\sim 760$  MHz, which corresponds to the expected combination of Doppler and pressure broadening (pressure broadening coefficient of  $\sim 9$  MHz/mbar) [30]. Using the modulated, amplified diode laser, the absorption linewidth in the gas cell and hollow core fiber are measured to be  $\sim 765$  MHz and 545 MHz respectively. From the results, we determine that the linewidth of the modulated amplified diode laser is  $< 100$  MHz. The absorption coefficient, defined as the ratio of the absorbed energy at the central wavelength to the transmitted energy when the wavelength is out of the absorption band, in the gas cell is  $\sim 0.78$ , and due to the longer interaction length in the hollow core fiber is  $\sim 0.95$ ,

which means that the ASE has been strongly suppressed in the EDFAs. All the central wavelengths are nearly identical, as the frequency shift induced by the pressure is very small, about  $-0.22$  MHz/mbar [30].

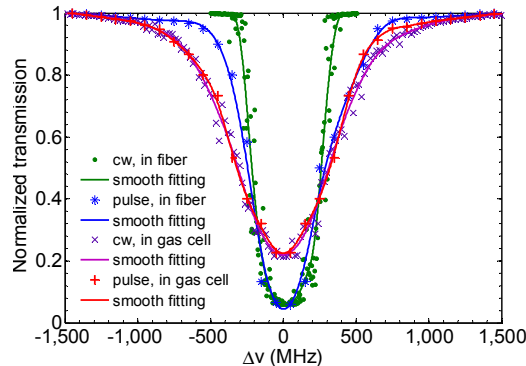


Fig. 3. The measured acetylene ( $^{12}\text{C}_2\text{H}_2$ ) absorption linewidth, the discrete points is the measured data, and the solid lines are the corresponding fitting curves respectively.

### 2.3 Acetylene-filled HC-PCF laser configuration

The total experimental setup is shown in Fig. 4. The incident pump power is controlled using a continuously tunable attenuator. About 3% of the total power is sent to a power meter through two beam splitters, used as the incident power monitor; about 1% is sent to the acetylene reference gas cell. A quarter-wave plate and a half-wave plate are used to optimize the transmitted power as the fiber loss is slightly polarization-dependent. The pump beam is focused into the hollow core fiber through a plano-convex lens (focal length 50 mm, anti-reflection coating 1050-1620 nm, measured transmission  $\sim 98\%$  at 1530 nm) and a silica window (anti-reflection coating 1050-1620 nm, measured transmission  $>98\%$  at 1530 nm).

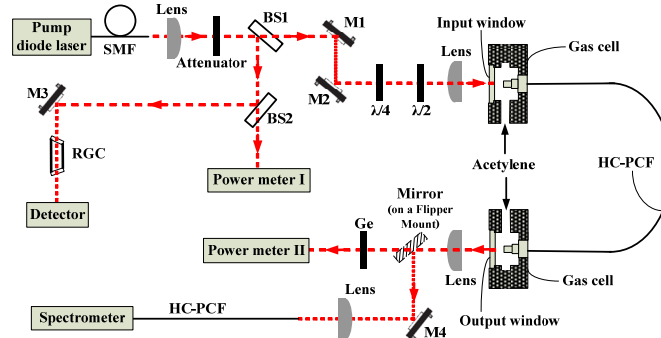


Fig. 4. Acetylene-filled HC-PCF laser setup. SMF: Single-mode fiber; BS: Beam splitter; M: Mirror;  $\lambda/4$ : Quarter-wave plate;  $\lambda/2$ : Half-wave plate; RGC: Acetylene reference gas cell; Ge: Germanium filter; DAQ: Data acquisition card; PC: Personal computer.

The optimized coupling efficiency is estimated to be 80%. The laser output (and the residual pump) passes through an uncoated sapphire window (transmission  $\sim 86\%$  at both pump and laser wavelengths), and is collimated by a calcium fluoride ( $\text{CaF}_2$ ) plano-convex lens (focal length 50 mm, anti-reflection coating 3-5  $\mu\text{m}$ , measured transmission  $\sim 97\%$  at 3.1-3.2  $\mu\text{m}$ ). The collimated beam is then sent to another thermal power meter passing through a germanium filter, or delivered to a spectrometer by a similar hollow core fiber. The gain fiber is filled with acetylene (with natural isotope ratio) using two gas cells. We waited several hours for the acetylene pressure in the fiber to equilibrate.

### 3. Experimental results and discussion

The output optical spectrum is shown in Fig. 5(a). It can be seen that the laser emission has two strong peaks near 3.12  $\mu\text{m}$  and 3.16  $\mu\text{m}$ , which match well with the expected wavelengths of R(7) and P(9) transition from vibrational state  $\nu_1 + \nu_3$  to  $\nu_1$  in  $^{12}\text{C}_2\text{H}_2$ , as shown in Fig. 5(b). Acetylene molecules are excited from the  $j = 9$  rotational state of the vibrational ground state to the  $j = 8$  rotational state of  $\nu_1 + \nu_3$  vibrational state by the pump pulses. The molecules can leave  $\nu_1 + \nu_3$  state through radiative transition to  $\nu_1$  vibrational state. According to the selection rules, the destination energy levels could be  $j = 7$  and 9 rotational states, corresponding to R(7) and P(9) respectively and these are the two lasing lines. Alternatively, the excited molecules may transit to  $\nu_1$  state nonradiatively due to intermolecular collisions or collisions with the fiber core wall, which will decrease the laser efficiency. At pressures above 2.5 mbar, the calculated mean free path (MFP) of acetylene molecules is  $<30 \mu\text{m}$ , which is much smaller than the core size of the fiber, so the intermolecular collisions are dominant. At pressures below 0.4 mbar, the MFP will be  $>100 \mu\text{m}$ , and so the contribution of wall collisions cannot be neglected. Because acetylene molecules cannot spontaneously go back to the ground vibrational state from  $\nu_1$  state, pulsed pumping is required for effective emission.

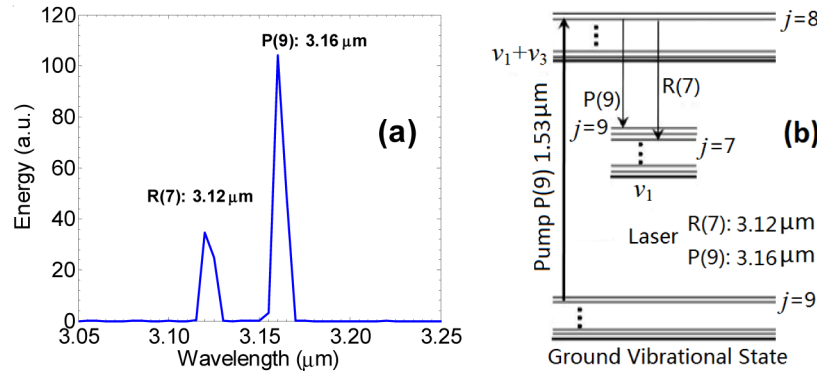


Fig. 5. (a) Measured output optical spectrum of  $^{12}\text{C}_2\text{H}_2$  at 0.7 mbar pressure, 10.5 m length, and 4.2  $\mu\text{J}$  incident pump energy; (b) Simple energy levels diagram of  $^{12}\text{C}_2\text{H}_2$  showing the pump and laser transitions.

The total laser power output of 10.5 m fiber with different incident pump powers and acetylene pressures was measured using a Germanium filter (the measured transmission coefficient at laser emission is 58%, and the loss at pump wavelength is  $>30 \text{ dB}$ ). The measured laser energy with total incident pump pulse energy of 4.2  $\mu\text{J}$  at different acetylene pressures is shown in Fig. 6(a). It can be seen that the optimum pressure is  $\sim 0.7 \text{ mbar}$ , which is in agreement with the calculated value 0.6 mbar using the model in Ref [20]. and [22]. From Fig. 6(b), it can be seen that the laser pulse energy increases nearly linearly with the absorbed pump pulse energy beyond the threshold. The minimum pump required to observe an output was below 50 nJ at 0.7 mbar, while the maximum output average laser power is  $\sim 7.6 \text{ mW}$  corresponding to  $\sim 0.76 \mu\text{J}$ . The energy conversion efficiency (the ratio of the laser pulse energy to the absorbed pump pulse energy), is calculated from the data in Fig. 6(b), as shown in Fig. 6(c). It can be seen that the conversion efficiency increases sharply at low pump energies, and the growth rate decreases with the further increase in the absorbed pump energy, approaching saturation at high energies. A maximum energy conversion efficiency of  $\sim 30\%$ , is obtained at 0.7 mbar, and the maximum conversion efficiency with respect to the total incident pump energy is  $\sim 20\%$ , which is limited by the effects of the ASE and pump linewidth. Because we are able to use a long length of low-loss fiber we do not see any saturation of output energy at high pump power, even at low pressure, allowing the highest output energy and highest efficiency to be attained simultaneously. Previous reports [20,21]

achieved high conversion efficiency only up to  $\sim 1$   $\mu\text{J}$  absorbed pump energy. The total optical-to-optical efficiency could be improved by further suppressing the ASE using a narrow-band filter before the power-amplifier, reducing the pump laser linewidth using more highly doped and shorter erbium fibers in the power-amplifier.

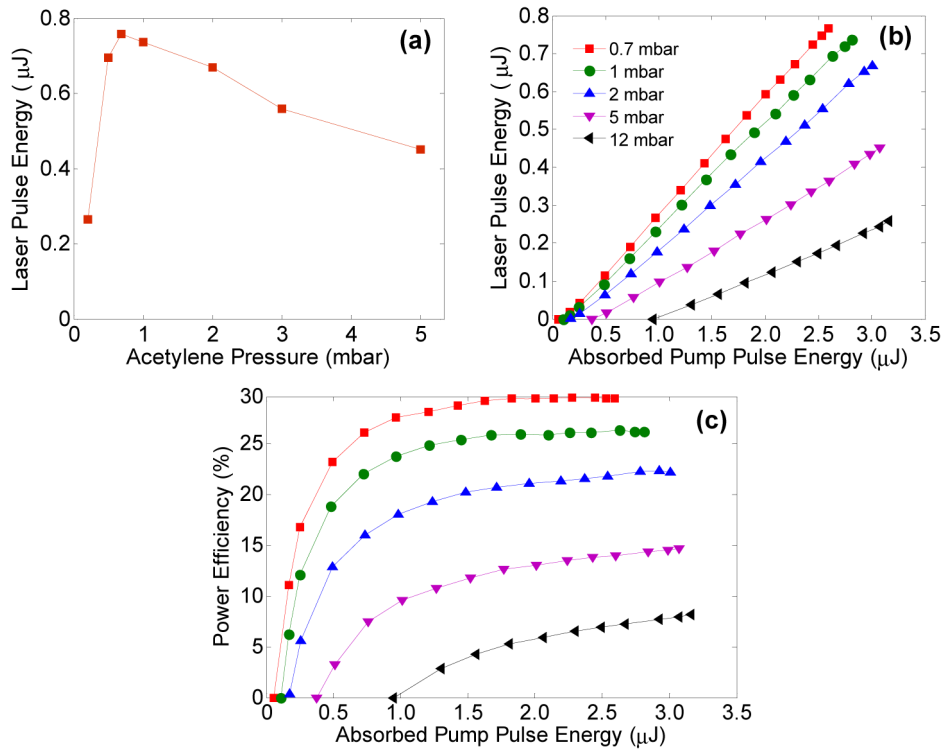


Fig. 6. (a) Measured output laser pulse energy with acetylene pressure, and the total incident pump pulse energy is  $\sim 4.2$   $\mu\text{J}$ ; (b) Output laser emission pulse energy is plotted versus the absorbed pump pulse energy at different acetylene pressure; (c) The evolution of the power conversion efficiency with respect to the absorbed pump pulse energy, from top to bottom corresponding to 0.7 mbar, 1 mbar, 2 mbar, 5 mbar, 12 mbar respectively.

#### 4. Conclusions

Using low-loss antiresonant hollow core fibers filled with acetylene, we have demonstrated efficient diode-pumped 3.1-3.2  $\mu\text{m}$  mid-IR emission. The efficiency with respect to the total incident pump power is  $\sim 20\%$ , the minimum pump laser energy is  $< 50$  nJ, and no saturation of the output pulse energy is seen at our maximum pump energy of 3  $\mu\text{J}$ , which are substantial improvements over the similar results published previously [20–22] using an OPO as pump source. Due to the low transmission loss, large core size and high damage threshold of the antiresonant hollow core fibers, efficient, compact, high-power mid-IR fiber gas lasers can potentially be obtained at a number of wavelengths by properly designing the fiber's transmission bands, and carefully selecting active gases and pump lasers.

#### Acknowledgment

This work is supported by the UK Engineering and Physical Sciences Research Council (EP/I011315/1), the International Science & Technology Cooperation of China (2012DFG11470), and National Natural Science Foundation of China (11274385).